A correction method for the loss of sensitivity of the LWR camera from 1978 to 1983

J. Clavel, R. Gilmozzi and A. Prieto

1. Introduction

It has been suggested several times that the LWR camera has suffered from a steady decline of its sensitivity since IUE was launched, January 26, 1978 (eg Sonneborn, 1984). Holm (1985) attempted a quantification of this effect as a function of wavelength and time. However, the data base he used was restricted to a small number (29) of low dispersion spectra of calibration stars. In addition, since the sampling rate he used was much smaller than that of the LWR calibration table (50 Å), the final curve he obtains is extremely noisy. It does suggest however that the rate at which the sensitivity dropped varies on a short wavelength scale. Moreover, his study included small aperture as well as trailed data which are known to yield slight discrepancies in the derivation of the fundamental sensitivity curve of the IUE instrument.

Given the amplitude of the sensitivity loss indicated by this and other studies and the impact this is bound to have both on long term monitoring projects of variable astronomical sources and on the calibration of future UV experiments, it was decided to undertake a more systematic investigation of this effect.

The aim of this paper is to provide a definitive correction method intended to bring all LWR low dispersion calibrated spectra on the same sensitivity scale.

We have analysed all the low-resolution spectra of the main IUE calibration stars obtained since launch up to 1983 (when the camera was turned-off) and derived the loss of sensitivity of the LWR camera both as a function of time and wavelength.
We have restricted our analysis to those stars faint enough to be observed in a point-source mode but with exposure times long enough to be accurate to better than 1 %. We present here the results of our study, together with a method for correcting for drop of sensitivity of the LWR camera.

2. The data base and its analysis

All the low dispersion large aperture spectra of the 5 main IUE calibration stars have been retrieved from the data bank. This includes 64 spectra of BD+28 424, 77 of HD 60753, 52 of BD+33 2642, 51 of BD+75 325 and 64 of HD 93521. All images have been processed (or reprocessed whenever necessary) with the new low dispersion software. The analysis itself was performed with the ESO IHAP system installed at VILSPA. Each star was analysed separately and it is only at a later stage that the various data sets were combined. In this way we are able to disentangle systematic effects which could be due, for instance, to the difference in spectral type.

The net fluxes were first averaged in bins of 50 Å, (coinciding with those of the LWR sensitivity curve) and the mean and standard deviation were computed for each spectrum and each bin, from 1850 Å up to 3300 Å, expanding our previous work carried out from 2000 Å up to 3200 Å (Clavel & Gilmozzi, 1984). These quantities were later divided by the exposure time and corrected for the thermal dependence of the LWR sensitivity, i.e. divided by:

$$1.0 - 0.011 * (THDA - 12)$$

(Shiffer, 1982; Bohlin & Holm, 1980). The exposure times t_{exp} were corrected for the rise time of the camera and the OBC timing, i.e.:

$$t_{exp} = 0.4096 * Int(t_{nom} / 0.4096) - 0.12 \quad (sec)$$

where t_{nom} is the nominal exposure time as given in the header, and Int (n) denotes the integer portion of number n.

We inspected each individual spectrum and removed the hot spot near 2190 Å, the reseaux marks, the most obvious blemishes and, when appropriate, the presence of microphonic noise. Following the results of our preliminary analysis (Clavel & Gilmozzi, 1984), we only included those spectra which had been obtained through the large aperture and with the nominal exposure time. No trailed spectra were analysed . After a quick-look at the basic trends, we also decided to reject the few spectra which gave clearly discrepant information (usually more than three sigmas out).

The final combined data set includes 308 spectra. For each star and each bin separately we plotted the net count rate, $C(\lambda,T)$ (IUE flux-numbers / sec) versus the time of acquisition, T . The launch-date, To, was taken as day 0. A linear regression analysis yielded:

$$C(\lambda,T) = Co(\lambda) + C1(\lambda) * T$$

The data were then normalized, i.e., divided by $Co(\lambda) = C(\lambda,To)$ which amounts to taking the count rate at launch as a reference value: Co = 1. A linear regression was performed again on the normalized data and yielded:

$$K(\lambda,T) = 1 + K1(\lambda) * T$$

The $K1(\lambda)$ values were later multiplied by 365 to obtain for each bin the rate of sensitivity loss in percentage per year. The results are listed in Table Ia for each star separately. The normalized data-sets for the five stars were merged and normalized again. Note that this second normalization never amounted to more than 0.6 %. A final regression analysis and multiplication by 365 yielded the results which are listed in column 3 of Table Ib. For comparison, we also give in column 2 the mean loss rates, i.e. the average of the results obtained separately for the five stars. Figure 1 shows an example of the decrease in the LWR count rate with time. Figure 2 represents the rate of sensitivity loss as a function of wavelength, $D(\lambda)$ (%/yr).

3. Results

The final $D(\lambda)$ curve as derived from the analysis of the 5 IUE standards, confirms the one obtained in our previous progress report where only two stars had been studied. It is also in very good agreement with the results by Holm (1985). As expected, the error-bars are rather large at the edges of the LWR wavelength range where the sensitivity is lower, but on the average the accuracy is of the order of 0.1 %. The small scale structure of the $D(\lambda)$ curve is confirmed.

It was assumed throughout that the degradation had been linear with time. There is some hint that this assumption is not entirely correct, since, irrespective of the wavelength, the data points around day 620 after launch (see fig. 1) for instance are systematically below the regression line. Nevertheless, the overall effect is sufficiently small (1%) that it can safely be ignored. Moreover, a more sophisticated functional representation of the temporal behaviour (e.g. a quadratic or higher order polynomial) would make the correction procedure somewhat cumbersome. Given the small amplitude of these non-linear trends and the intrinsic limitation due to the noise in the data, as well as for the sake of clarity, it was decided to retain a linear representation of the LWR sensitivity loss.

To correct for the degradation of the LWR performance, the following steps are recommended:

1/- First, to bring the $D(\lambda)$ function onto the IUE LWR wavelength scale, use a spline interpolation of the natural logarithm of the values listed in table Ib, column 3. A similar method of interpolation is used in Image Processing production to generate the IUE calibration file.

2/- The correction formula itself is straightforward:

$$F_{corr}(\lambda) = F(\lambda) \,/\, [1 - D(\lambda) * \Delta T]$$

$$\Delta T = T - 1978.8$$

where $F(\lambda)$ and $F_{corr}(\lambda)$ refer to the calibrated spectrum respectively before and after correction, and ΔT is the time which has elapsed since the IUE absolute calibration was established (mean epoch 1978.8). As an example, we have applied the above procedure to correct two spectra of BD+78 4211 obtained ~ four years apart (both corrected for THDA). Figures 3 & 4 show the percentage difference for the uncorrected and corrected spectra respectively. The difference, averaged over the 2000-3000 Å interval are respectively:

$- 8.7 \pm 9.6$ % (uncorrected)

$+ 0.08 \pm 10.2$ % (corrected)

4. Conclusion and future work

It has been found that the rate of sensitivity loss of the LWR camera varies on a short wavelength scale (50 Å). It reaches a maximum of 3.54 % / yr at 2300 Å. No systematic differences exist between the results obtained for the 5 stars separately. To a good approximation, the sensitivity decreased linearly with time, and therefore the results presented here can safely be applied to correct LWR spectra taken at different epochs. A similar analysis is planned for the SWP camera, though this instrument apparently did not suffer from such a large drop of its performance as the long wavelength detector (Sonneborn, 1984).

5. References

Bohlin,R., Holm,A., 1980, NASA IUE Newsletter 10, 37.*
Clavel,J.,Gilmozzi,R.,1984,3-A Meeting Report,GSFC November 1984.
Holm,A., 1985, NASA IUE Newsletter 26, 11.
Schiffer,F.H., 1982, NASA IUE Newsletter 19, 33.
Sonneborn,G., 1984, NASA IUE Newsletter 24, 67.

* (= ESA IUE Newsletter 11, 18)

TABLE I.a : Final results for the five stars separately. Sensitivity is expressed in percentage per year.

	Rate of decrease of sensitivity (%/yr)				
Wavelength	BD+28 4211	HD 60753	BD+33 2642	BD+75 325	HD 93521
1825-1875	1.56±0.79	3.36±0.82	5.67±1.29	3.44±0.74	2.83±1.30
1875-1925	2.00±0.45	2.53±0.36	- ± -	3.19±0.39	1.88±0.46
1925-1975	1.30+0.30	2.32+0.30	2.61+0.45	2.75+0.26	1.56+0.44
1975-2025	2.13±0.25	2.00±0.26	2.53±0.40	2.44±0.25	2.30±0.28
2025-2075	2.02±0.21	2.30±0.23	2.78±0.36	2.85±0.19	2.45±0.27
2075-2125	2.40±0.26	1.92±0.27	2.53±0.36	2.93±0.25	2.60±0.29
2125-2175	2.31±0.21	1.83±0.19	2.20±0.27	2.47±0.19	2.21±0.22
2175-2225	2.70±0.29	3.01±0.25	2.55±0.42	3.47±0.28	2.81±0.33
2225-2275	3.28±0.24	3.01±0.20	3.24±0.32	3.20±0.21	2.99±0.21
2275-2325	3.32±0.24	3.42±0.25	3.55±0.36	3.68±0.19	3.65±0.27
2325-2375	3.36±0.24	2.77±0.28	3.69±0.35	3.71±0.20	3.54±0.28
2375-2425	2.60±0.28	2.06±0.21	2.64±0.29	2.56±0.24	2.36±0.25
2425-2475	2.55±0.25	1.89±0.25	2.42±0.26	2.49±0.21	2.13±0.22
2475-2525	2.30±0.25	1.56±0.23	1.73±0.26	1.89±0.22	1.70±0.23
2525-2575	1.96±0.23	1.30±0.26	1.65±0.31	2.43±0.23	1.72±0.26
2575-2625	2.02±0.25	1.72±0.21	2.41±0.29	1.28±0.25	1.73±0.24
2625-2675	1.33±0.22	1.33±0.19	1.33±0.26	1.70±0.23	1.10±0.23
2675-2725	1.92±0.24	1.88±0.20	1.88±0.25	2.07±0.23	1.43±0.26
2725-2775	1.95±0.27	1.98±0.23	1.89±0.27	2.13±0.29	1.30±0.24
2775-2825	2.12±0.29	2.06±0.26	2.42±0.33	2.72±0.31	1.96±0.35
2825-2875	2.22±0.29	1.87±0.22	2.29±0.30	2.29±0.22	1.77±0.26
2875-2925	1.79±0.26	1.46±0.22	1.91±0.23	1.98±0.25	1.45±0.28
2925-2975	1.59±0.23	1.22±0.23	2.06±0.26	1.88±0.25	1.54±0.32
2975-3025	1.58±0.30	1.28±0.25	1.96±0.33	1.69±0.25	1.17±0.34
3025-3075	1.89±0.29	1.26±0.34	2.58±0.35	2.02±0.36	1.51±0.40
3075-3125	1.52±0.31	1.51±0.31	1.97±0.42	2.04±0.38	1.52±0.37
3125-3175	0.91±0.49	1.12±0.36	1.84±0.44	1.19±0.47	0.78±0.49
3175-3225	3.23±0.62	2.38±2.28	4.24±0.89	4.30±0.72	1.50±0.99
3225-3275	1.53±0.94	0.79±0.65	2.70±1.53	1.78±0.89	0.76±0.96
3275-3325	- ± -	0.11±1.15	0.01±2.47	2.18±1.60	1.52±0.37

Table I.b : Final results for merged data; for comparison, the results obtained by averaging the sensitivity losses found for individual stars are also given. To correct for the sensitivity loss, use numbers of column 3 ("merged").

Rate of sensitivity loss (%/yr)		
Wavelength	Average	merged
1825-1875	3.47±1.50	3.75±0.49
1875-1925	1.92±1.19	2.19±0.25
1925-1975	2.11±0.64	2.31±0.17
1975-2025	2.28±0.22	2.30±0.12
2025-2075	2.48±0.34	2.56±0.12
2075-2125	2.48±0.37	2.49±0.14
2125-2175	2.20±0.24	2.20±0.10
2175-2225	2.91±0.36	2.99±0.14
2225-2275	3.14±0.13	3.12±0.11
2275-2325	3.52±0.15	3.54±0.12
2325-2375	3.41±0.39	3.42±0.12
2375-2425	2.44±0.24	2.42±0.12
2425-2475	2.30±0.28	2.27±0.11
2475-2525	1.84±0.28	1.77±0.11
2525-2575	1.81±0.42	1.83±0.13
2575-2625	1.83±0.42	1.75±0.12
2625-2675	1.36±0.22	1.40±0.10
2675-2725	1.84±0.24	1.86±0.11
2725-2775	1.85±0.32	1.90±0.12
2775-2825	2.26±0.31	2.31±0.14
2825-2875	2.09±0.25	2.10±0.11
2875-2925	1.72±0.25	1.74±0.11
2925-2975	1.66±0.32	1.67±0.12
2975-3025	1.54±0.32	1.55±0.13
3025-3075	1.85±0.51	1.87±0.16
3075-3125	1.71±0.27	1.77±0.16
3125-3175	1.17±0.41	1.26±0.20
3175-3225	3.73±1.21	3.30±0.63
3225-3275	1.51±0.80	1.67±0.43
3275-3325	0.76±1.02	0.59±0.80

Figure 1 : Net 2300 A flux of the 5 calibration stars as a function of time. The fluxes have been normalized to 1000 at time of launch.

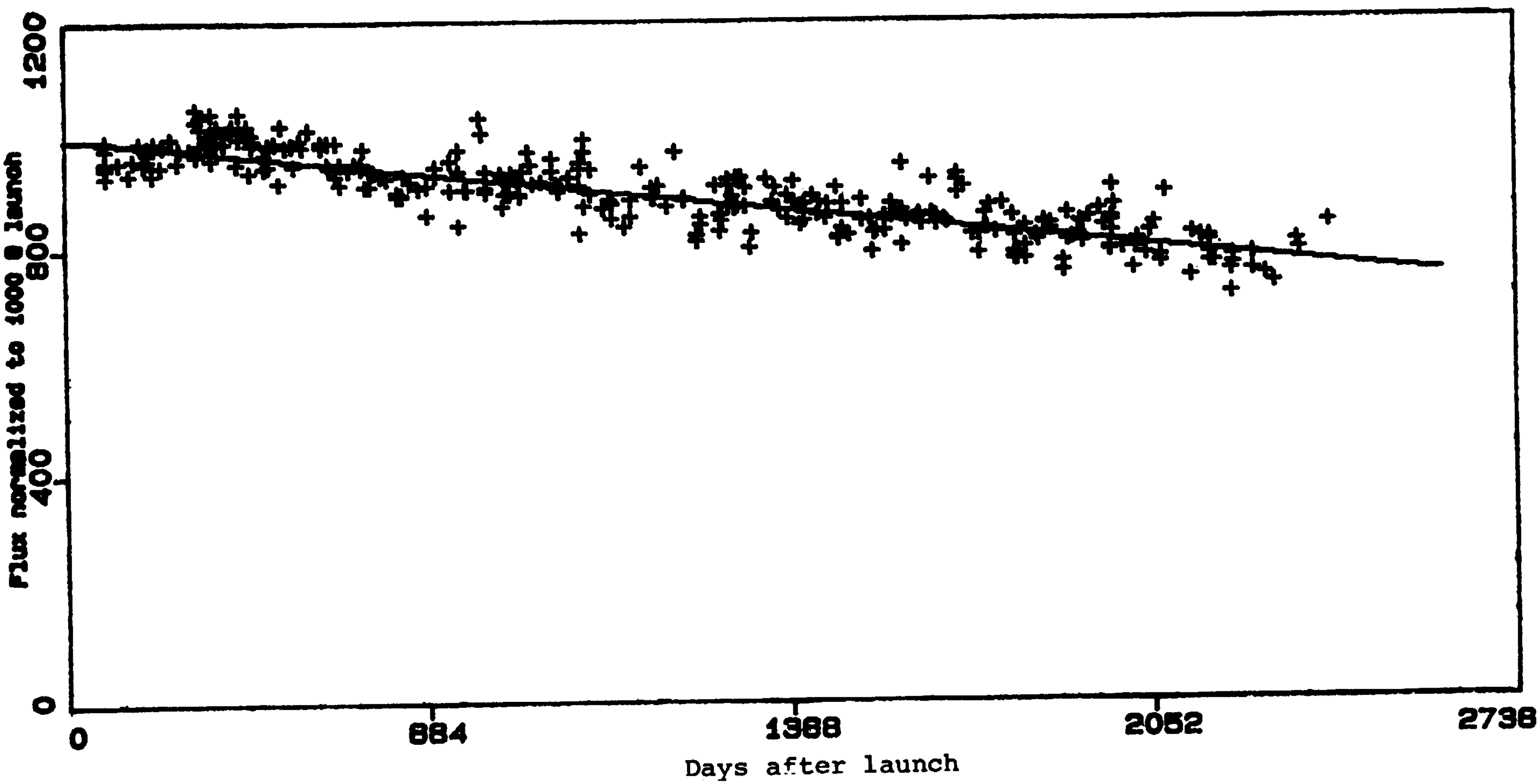

Figure 2 : The decrease in sensitivity of the LWR camera as a function of wavelength expressed in percentage per year.

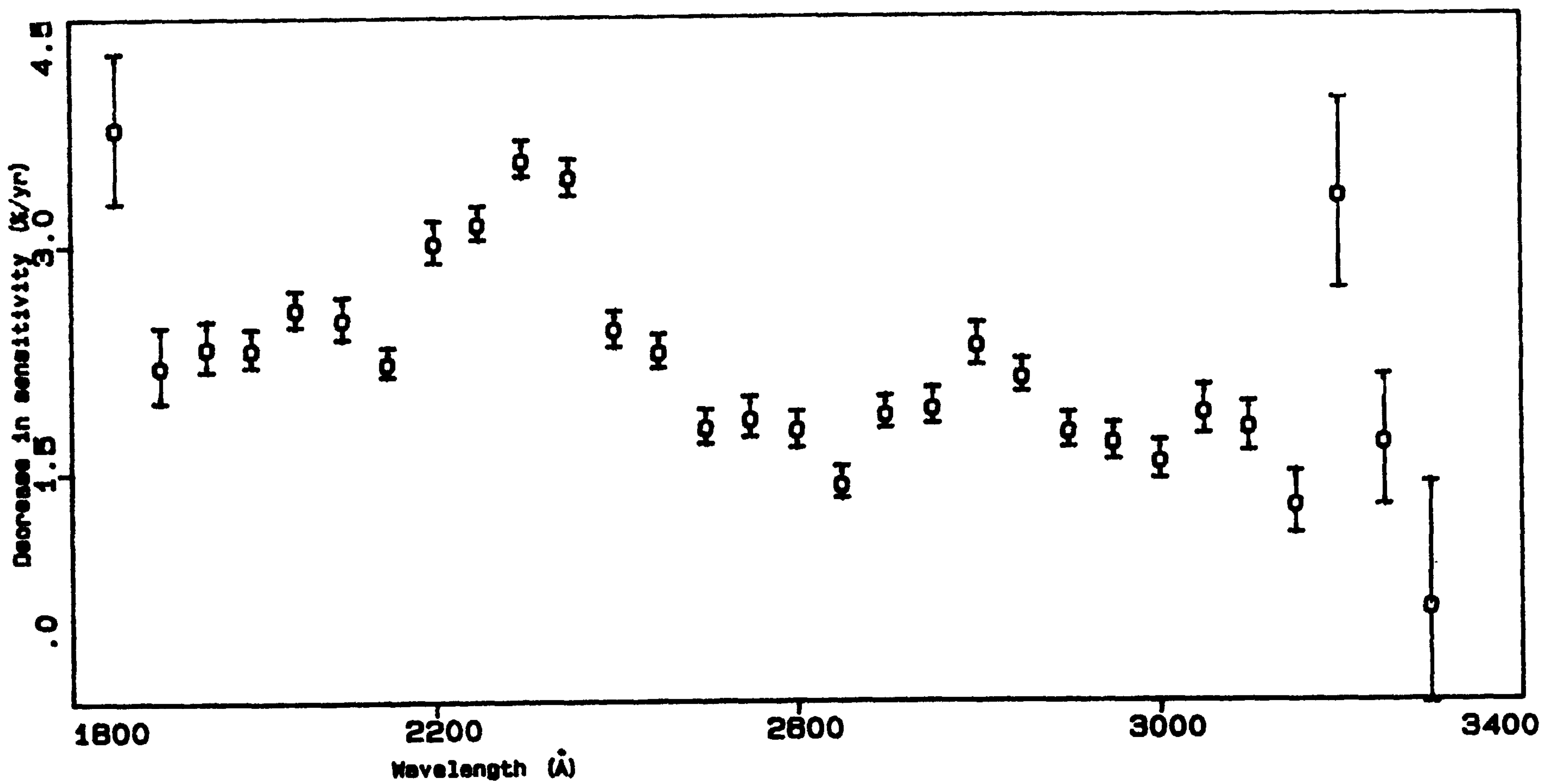

Figure 3 : Relative difference expressed in percentage between two spectra of BD+28 4211 taken approximately four years apart. Both spectra have been corrected for THDA. The difference averaged over the 2000-3000 A range amounts to 8.7 ± 9.6 %.

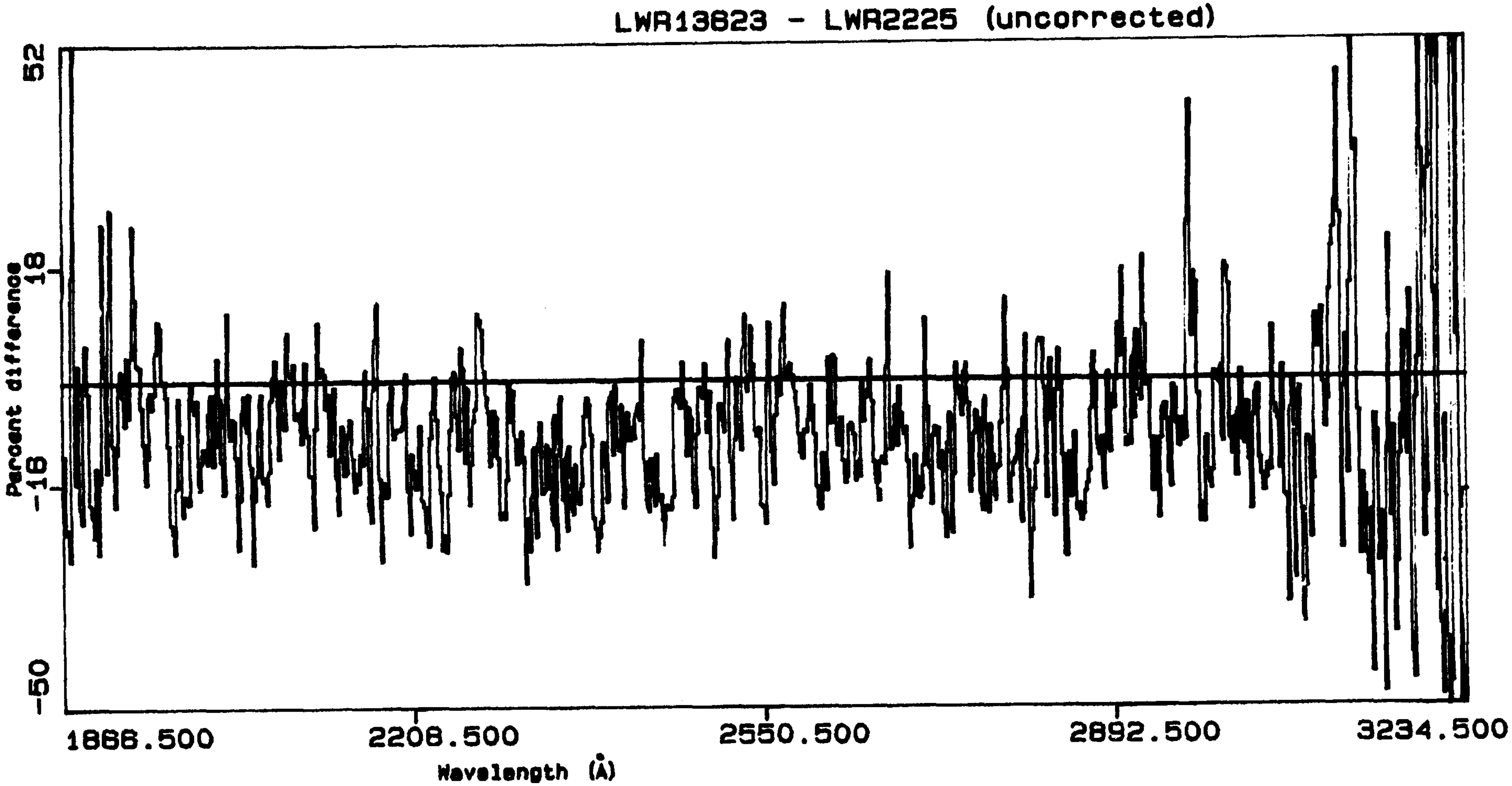

Figure 4 : Relative difference as a function of wavelength between the same spectra of BD+28 4211 as in the previous figure after correction for the sensitivity loss of the LWR camera. The average difference in the 2000-3000 A range is reduced to 0.08 ± 10.2 %.